ARTICLES

Journal of Semiconductors
(2020) 41, 102102
doi: 10.1088/1674-4926/41/10/102102

First principles study of the electronic structure and photovoltaic properties of β-$CuGaO_2$ with MBJ + U approach

Guoping Luo[1], Yingmei Bian[1], Ruifeng Wu[1], Guoxia Lai[1], Xiangfu Xu[1], Weiwei Zhang[2], and Xingyuan Chen[1, †]

[1]Department of Applied Physics, School of Science, Guangdong University of Petrochemical Technology, Maoming 525000, China
[2]School of Materials Science and Engineering, Chang'an University, Xi'an 710064, China

Abstract: Based on the density functional theory, the energy band and electronic structure of β-$CuGaO_2$ are calculated by the modified Becke-Johnson plus an on-site Coulomb U (MBJ + U) approach in this paper. The calculated results show that the band gap value of β-$CuGaO_2$ obtained by the MBJ + U approach is close to the experimental value. The calculated results of electronic structure indicate that the main properties of the material are determined by the bond between Cu-3d and O-2p energy levels near the valence band of β-$CuGaO_2$, while a weak anti-bond combination is formed mainly by the O-2p energy level and Ga-4s energy level near the bottom of the conduction band of β-$CuGaO_2$. The β-$CuGaO_2$ thin film is predicted to hold excellent photovoltaic performance by analysis of the spectroscopic limited maximum efficiency (SLME) method. At the same time, the calculated maximum photoelectric conversion efficiency of the ideal $CuGaO_2$ solar cell is 32.4%. Relevant conclusions can expand β-$CuGaO_2$ photovoltaic applications.

Key words: first principles; β-$CuGaO_2$; electronic structure; photovoltaic properties

Citation: G P Luo, Y M Bian, R F Wu, G X Lai, X F Xu, W W Zhang, and X Y Chen, First principles study of the electronic structure and photovoltaic properties of β-$CuGaO_2$ with MBJ + U approach[J]. *J. Semicond.*, 2020, 41(10), 102102. http://doi.org/10.1088/1674-4926/41/10/102102

1. Introduction

Oxide semiconductors generally have large band gaps, which can be widely used in thin-film transistors of the ultraviolet region, light-emitting diodes or transparent electrodes, etc.[1, 2]. Most oxide semiconductors are not suitable for applications in solar cells and photocatalysis because they are almost transparent to visible light. Hexagonal ZnO and anatase TiO_2 are typical oxide semiconductor materials with band gaps of 3.37 and 3.2 eV, respectively[3, 4]. However, the band gaps of Cu_2O and wurtzite-derived $AgGaO_2$ are approximately 2 eV, which can be used to prepare solar cells and photocatalytic materials[5, 6]. In 2014, Omata *et al.* of Osaka University prepared β-$CuGaO_2$ oxide semiconductors by ion replacement of $NaGaO_2$ materials[7]. β-$CuGaO_2$ is a direct bandgap material with a band gap of 1.47 eV, which is very beneficial for the preparation of a new type of photovoltaic material. Song *et al.* believe that β-$CuGaO_2$ also has ferroelectricity and could be potential ferroelectric photovoltaic materials by DFT research[8]. Currently, the popular ferroelectric photovoltaic materials such as $BaTiO_3$ and $BiFeO_3$ hold relatively large band gaps, low absorption of visible light, and low current density[9, 10], while β-$CuGaO_2$ are expected to absorb more visible light to improve the efficiency of ferroelectric photovoltaics. Okumura *et al.* found that Cu vacancies as p-type intrinsic defect could be easily emerged in β-$CuGaO_2$, and easily formed heterojunction semiconductors with ZnO[11]. It is necessary to introduce the Coulomb interaction parameter U into the Cu element to calculate the electronic structure for the 3d orbital of Cu ions is much localized and the traditional LDA and GGA calculated methods will underestimate the band gap[12]. However, Suzuki *et al.* calculated the band gap of β-$CuGaO_2$ with 0.3 eV by LDA + U (U = 6 eV) method, which is much smaller than the experimental band gap value of 1.47 eV[13]. The hybrid functional HSE and quasi-particle self-consistent GW are generally available for the accurate electronic structure relatively[14–16]. Okumura *et al.* calculated the band gap of β-$CuGaO_2$ by HSE method, and found that the band gap of β-$CuGaO_2$ is 1.09, 1.21, 1.56, and 1.96 eV respectively with the variational parameter α[11]. The band gap of 1.56 eV is the closest to the experimental value when the α parameter is 0.35[11]. They also calculated the band gap of β-$CuGaO_2$ with 0.84 eV by using the GW approach, which also deviated from the experimental value[11]. Furthermore, the computational costs of HSE and GW approach are relatively high. In this paper, the GGA + U and MBJ + U approach with low calculated cost have been employed to calculate the electronic structure of β-$CuGaO_2$, and found that the calculated band gap obtained by MBJ + U approach is very close to the experimental value. On the basis of electronic structure calculation by MBJ + U approach, the spectroscopic limited maximum efficiency (SLME)[17] method was also used to calculate the photovoltaic properties of β-$CuGaO_2$.

2. Theoretical model and calculated method

The calculations in this paper are carried out by the Vienna ab-initio simulation package (VASP) software package based on the density functional theory (DFT) theory[18, 19]. We used the PBE functional[20] within the generalized gradient approximation (GGA) for exchange–correlation interactions. The

Correspondence to: X Y Chen, chenxingyuan@gdupt.edu.cn
Received 12 DECEMBER 2019; Revised 13 JANUARY 2020.

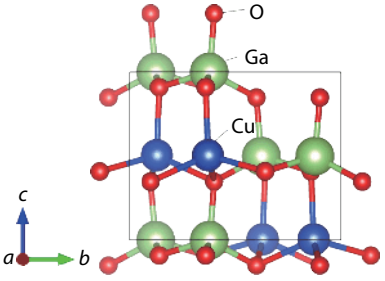

Fig. 1. (Color online) The structure of the β-$CuGaO_2$.

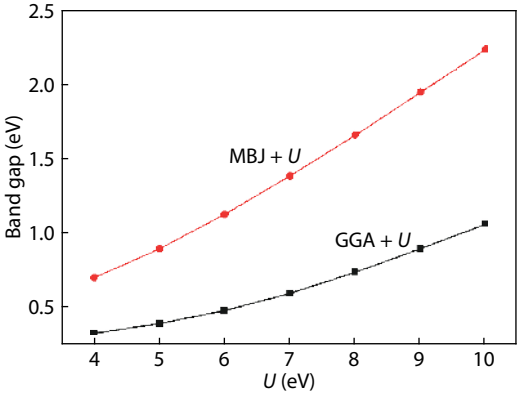

Fig. 2. (Color online) The band gap values of β-$CuGaO_2$ by GGA + U and MBJ + U method.

cut-off energy is set to 520 eV and the K-point sampling in the Brillouin zone is adopted to 6 × 5 × 6. The energy convergence standard is 10^{-6} eV and the Hellmann–Feynman force convergence criterion is less than 0.01 eV/ Å. The structure of β-$CuGaO_2$ is shown in Fig. 1. The calculated lattice parameters (a = 5.55 Å, b = 6.69 Å, c = 5.32 Å) are closed to the experimental values (a = 5.46 Å, b = 6.61 Å, c = 5.27 Å)[7] by GGA-PBE functional. The 2H (hexagonal) and 3R (trigonal) $CuGaO_2$ are usually stable structures. The space group of the 2H phase is $P6_3/mmc$ (No. 194) and 3R phase belongs to R-3m (No. 166) space group. The calculated energy difference between 2H and 3R $CuGaO_2$ is in the range of 5 meV/formula by GGA calculations. The β-$CuGaO_2$ belongs to $Pna2_1$ space group (No. 33). The calculated energy of β-$CuGaO_2$ are higher than 2H and 3R $CuGaO_2$ with about 60 meV/formula. The β-$CuGaO_2$ could be a substable structure. To obtain more accurate electronic structure, the coulomb interaction parameter U[21] is added to treat the 3d orbital of Cu element based on the calculated structure of GGA-PBE functional. Based on the framework of density functional calculation, the modified Becke-Johnson potential plus an on-site Coulomb U (MBJ + U)[21–23] approach was used to calculate the band structure and electronic structure of β-$CuGaO_2$. Our calculated band gap of β-$CuGaO_2$ obtained by MBJ + U approach is much closed to the experimental value. In a similar situation, the Cu-based material Cu_2X (X = S, Se, Te) is also calculated by MBJ + U to obtain accurate band gap and electronic structure[24].

3. The calculated results and discussion

3.1. The band structure and electronic structure

As shown in Fig. 2, the calculated band gap value does not exceed 1 eV by GGA + U with the values of U changing from 4 to 10 eV, which is deviated from the experimental value of 1.47 eV. However, in the calculations of MBJ + U approach, the calculated band gap value is very close to the experimental value when U takes 7 and 8 eV. Finally, we select MBJ + U (U = 7.3 eV) approach, and the calculate band gap value of β-$CuGaO_2$ is 1.46 eV. In the calculation of the latter electronic structure, we all take the parameters of MBJ + U (U = 7.3 eV), which ensures the reliability of our calculation.

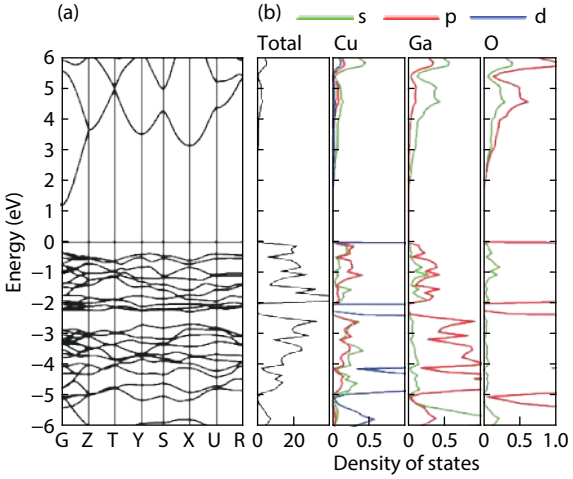

Fig. 3. (Color online) The band structure and DOS of β-$CuGaO_2$.

As shown in Fig. 3, the valence-band maximum (VBM) and the conduction band bottom (CBM) of β-$CuGaO_2$ are both at the G point, which indicated a direct band gap material. The curve near VBM is relatively flat, indicating that the effective mass of the hole is relatively large, while the effective mass of electrons is relatively small since the curve near CBM is steep, which is consistent with the early reported results[11, 13]. The valence band level of β-$CuGaO_2$ is mainly caused by the Cu-3d energy level and the O-2p energy level and the hybridization between Cu-3d energy level and the O-2p energy level determines the main properties of the material. The density of states (DOS) is relatively small to form a weak antibonding orbital between O-2p energy level and Ga-4s energy level near the conduction band of β-$CuGaO_2$. The transitions from the Cu-3d level to the O-2p energy level and the O-2p energy level to the Ga-4s energy level are prone to occur in β-$CuGaO_2$. These major energy level transitions will mainly affect the main optoelectronic properties of β-$CuGaO_2$.

3.2. Optical properties

The absorption coefficients [$\alpha(E)$] of β-$CuGaO_2$ were obtained by the following formula:

$$\alpha(E) = \frac{2\omega}{c}\left[\frac{\sqrt{\varepsilon_r(E)^2 + \varepsilon_i(E)^2} - \varepsilon_r(E)^2}{2}\right]^{1/2}, \quad (1)$$

where c is the speed of light in vacuum, ω is the incident light frequency. The imaginary and real parts of the dielectric function are expressed in terms of ε_i and ε_r, respectively. Fig. 4 shows the calculated absorption coefficients spectrum of β-$CuGaO_2$. The AM 1.5 solar spectral irradiance in the 300–1000 nm wavelength range is also shown in Fig. 4. It can see that β-$CuGaO_2$ exhibit high absorption coefficient up to 10^5 cm^{-1} in the visible region. The total fractional absorption

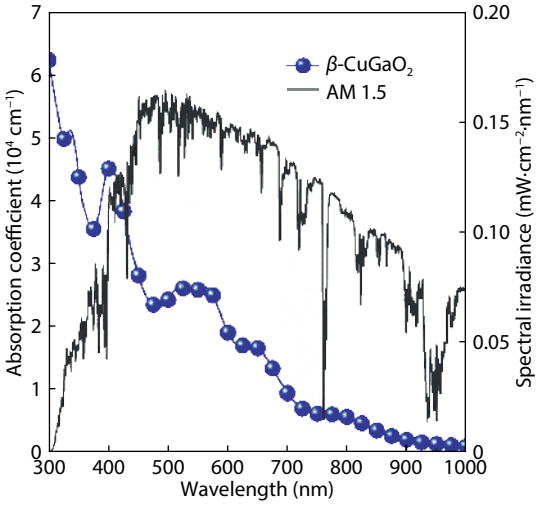

Fig. 4. (Color online) The absorption coefficient of β-$CuGaO_2$ and AM 1.5 solar spectral irradiance in the 300–1000 nm wavelength range.

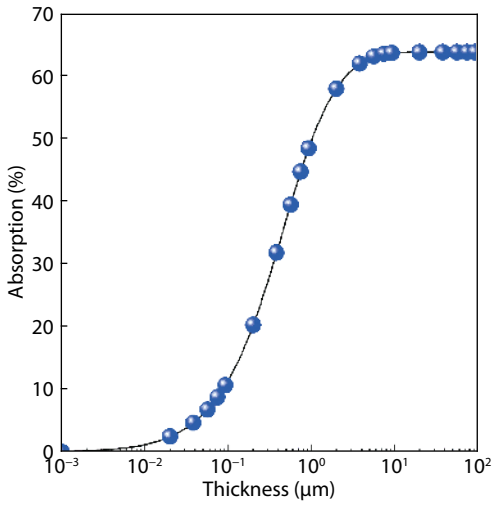

Fig. 5. (Color online) The optical absorption properties of β-$CuGaO_2$.

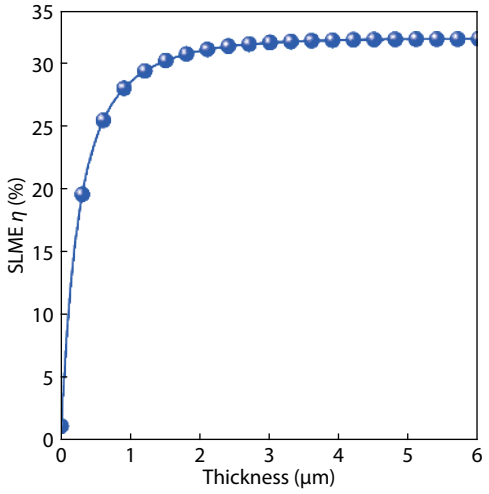

Fig. 6. (Color online) The SLME η as a function of film thickness for ideal β-$CuGaO_2$ solar cell.

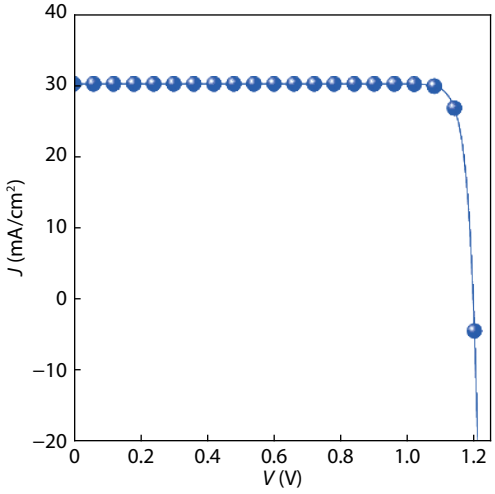

Fig. 7. (Color online) The current density–voltage (J–V) curves of the ideal β-$CuGaO_2$ solar cell with a thickness of 3 μm.

(A) of incident solar radiation can be approximately expressed as following formula with the film thickness (d) and absorption coefficient [$\alpha(E)$].

$$A(\%) = \left(1 - \frac{\int_0^{E_g} S_E \mathrm{d}E}{\int_0^{\infty} S_E \mathrm{d}E} - \frac{\int_{E_g}^{\infty} e^{-\alpha(E)\cdot d} S_E \mathrm{d}E}{\int_0^{\infty} S_E \mathrm{d}E}\right) \times 100, \quad (2)$$

where E_g is the band gap and S_E is the incident solar spectral irradiance changing with incident photon energy E. As film thickness of β-$CuGaO_2$ changes, the calculated fraction absorption of incident solar flux is shown in Fig. 5. As the thickness of β-$CuGaO_2$ thin films increases from 0.1 to 1 μm, the total fractional absorption slightly increased, and then starts to saturate with thickness of 3 μm.

3.3. Photovoltaic properties

The Shockley-Queisser limit indicates an absorber with bandgap nearby 1.4 eV has higher photovoltaic conversion efficiency[25]. The calculated bandgap of β-$CuGaO_2$ is 1.47 eV, showing that this material has the potential to an efficiency solar cell absorber. However, the thickness of the absorber layer, visible light absorption coefficient and carrier recombination are also important factors to the real cells' efficiency. Therefore, the photovoltaic properties of β-$CuGaO_2$ are estimated by the spectroscopic limited maximum efficiency (SLME) metric proposed by Yu and Zunger[17]. The SLME efficiency for β-$CuGaO_2$ thin films is shown in Fig. 6 with a function of thickness. We find that the SLME efficiency first increases rapidly with increasing film thickness. This mainly attribute to the increasing of film absorption. The SLME efficiency achieves maximum value as high as 32% at large film thickness. A layer thickness L = 3.0 μm is considered for the SLME calculation since beyond that value the efficiency is not noticeably changed whereas below that value. The typical current density–voltage (J–V) curves for the β-$CuGaO_2$ are shown in Fig. 7. The photovoltaic parameters can be derived from Fig. 7, as shown in Table 1. For comparison, the photovoltaic parameters of theoretically and experimentally CdTe solar cells are also given in Table 1. Even though the open circuit voltage (V_{oc}) of β-$CuGaO_2$ based photovoltaics cells is lower than the value of CdTe, but the conversion efficiency (η) and short circuit current density (J_{sc}) are much higher. These calculated results indicate that β-$CuGaO_2$ is a candidate for use as a highly efficient photovoltaic absorber material.

Table 1. The photovoltaic parameters of β-$CuGaO_2$ and CdTe solar cells obtained by SLME method, the experimentally parameters for CdTe solar cells are also included for comparison.

Absorber	V_{oc} (V)	J_{sc} (mA/cm^2)	η (%)
β-$CuGaO_2$ (SLME)	1.20	30.2	32.4
CdTe (SLME)[26]	1.30	23.0	27.0
CdTe (EXP)[27]	0.87	26.0	20.4

4. Conclusions

In summary, GGA + U and MBJ + U approach with lower calculated costs are employed to calculate the electronic structure of β-$CuGaO_2$ in this paper. It is found that the calculated band gap value obtained by MBJ + U (U = 7.3 eV) approach is closer to the experimental value. Near the top of the valence band of β-$CuGaO_2$ is mainly composed of the Cu-3d energy level and the O-2p energy level. The bond formed by the hybridization between Cu-3d energy level and the O-2p energy level determines the main properties of the material. When the thickness of β-$CuGaO_2$ film is increased from 0.1 to 1 μm, the total absorption of the film increases sharply. The total absorption becomes to saturation when the film thickness is about 3 μm. The photovoltaic performance parameters of idea β-$CuGaO_2$ solar cells are calculated by the SLME method, which indicated that it could reach 32.4% energy conversion efficiency. By comparison with photovoltaic parameters of CdTe thin film solar cells, it was found that β-$CuGaO_2$ could be a potential high-efficiency photovoltaic material.

Acknowledgements

This work was supported by the NSFC (Grant No. 11547201), Natural Science Foundation of Guangdong Province, China (Grant No. 2017A030307008), Natural Science Basic Research Program of Shaanxi (Program No. 2019JQ-380), and Natural Science Foundation of Guangdong Petrochemical University of Technology, China (Grant No. 2017rc20).

References

[1] Ellmer K. Past achievements and future challenges in the development of optically transparent electrodes. Nat Photonics, 2012, 6(12), 809
[2] Minami T. Transparent conducting oxide semiconductors for transparent electrodes. Semicond Sci Tech, 2005, 20(4), S35
[3] Klingshirn C. The luminescence of ZnO under high one- and two-quantum excitation. Phys Status Solidi B, 1975, 71(2), 547
[4] Tang H, Prasad K, Sanjines R, et al. Electrical and optical properties of TiO_2 anatase thin films. J Appl Phys, 1994, 75(4), 2042
[5] Baumeister P W. Optical absorption of cuprous oxide. Phys Rev, 1961, 121(2), 359
[6] Omata T, Nagatani H, Suzuki I, et al. Wurtzite-derived ternary I–III–O_2 semiconductors. Sci Tech Adv Mater, 2015, 16(2), 024902
[7] Omata T, Nagatani H, Suzuki I, et al. Wurtzite $CuGaO_2$: A new direct and narrow band gap oxide semiconductor applicable as a solar cell absorber. J Am Chem Soc, 2014, 136(9), 3378
[8] Song S, Kim D, Jang H M, et al. β-$CuGaO_2$ as a strong candidate material for efficient ferroelectric photovoltaics. Chem Mater, 2017, 29(17), 7596
[9] Berglund C N, Braun H J. Optical absorption in single-domain ferroelectric barium titanate. Phys Rev, 1967, 164(2), 790
[10] Ji W, Yao K, Liang Y C. Bulk photovoltaic effect at visible wavelength in epitaxial ferroelectric $BiFeO_3$ thin films. Adv Mater, 2010, 22(15), 1763
[11] Okumura H, Sato K, Kakeshita T. Electronic structure, defect formation energy, and photovoltaic properties of wurtzite-derived $CuGaO_2$. J Appl Phys, 2018, 123(16), 161584
[12] Wang L, Maxisch T, Ceder G. Oxidation energies of transition metal oxides within the GGA + U framework. Phys Rev B, 2006, 73(19), 195107
[13] Suzuki I, Nagatani H, Kita M, et al. First principles calculations of ternary wurtzite β-$CuGaO_2$. J Appl Phys, 2016, 119(9), 095701
[14] Heyd J, Scuseria G E, Ernzerhof M. Hybrid functionals based on a screened Coulomb potential. J Chem Phys, 2003, 118(18), 8207
[15] Shishkin M, Kresse G. Implementation and performance of the frequency-dependent GW method within the PAW framework. Phys Rev B, 2006, 74(3), 035101
[16] Hafner J. Ab-initio simulations of materials using VASP: Density-functional theory and beyond. J Comput Chem, 2008, 29(13), 2044
[17] Yu L, Zunger A. Identification of potential photovoltaic absorbers based on first-principles spectroscopic screening of materials. Phys Rev Lett, 2012, 108(6), 068701
[18] Kresse G, Furthmüller J. Efficiency of ab-initio total energy calculations for metals and semiconductors using a plane-wave basis set. Comput Mater Sci, 1996, 6(1), 15
[19] Kresse G, Joubert D. From ultrasoft pseudopotentials to the projector augmented-wave method. Phys Rev B, 1999, 59, 1758
[20] Perdew J P, Burke K, Ernzerhof M. Generalized gradient approximation made simple. Phys Rev Lett, 1996, 77, 3865
[21] Liechtenstein A I, Anisimov V I, Zaanen J. Density-functional theory and strong interactions: Orbital ordering in Mott-Hubbard insulators. Phys Rev B, 1995, 52(8), R5467
[22] Becke A D, Johnson E R. A simple effective potential for exchange. J Chem Phys, 2006, 124, 221101
[23] Tran F, Blaha P. Accurate band gaps of semiconductors and insulators with a semilocal exchange-correlation potential. Phys Rev Lett, 2009, 102(22), 226401
[24] Zhang Y, Wang Y, Xi L, et al. Electronic structure of antifluorite Cu_2X (X = S, Se, Te) within the modified Becke-Johnson potential plus an on-site Coulomb U. J Chem Phys, 2014, 140(7), 074702
[25] Shockley W, Queisser H J. Detailed balance limit of efficiency of p-n junction solar cells. J Appl Phys, 1961, 32(3), 510
[26] Huang X, Paudel T R, Dong S, et al. Hexagonal rare-earth manganites as promising photovoltaics and light polarizers. Phys Rev B, 2015, 92(12), 125201
[27] Green M A, Emery K, Hishikawa Y, et al. Solar cell efficiency tables (Version 45). Prog Photovolt: Res Appl, 2015, 23(1), 1